Introduction of thermal activation in forward modeling of hysteresis loops for single-domain magnetic particles and implications for the interpretation of the Day diagram

Luca Lanci[1] and Dennis V. Kent[2]

Geological Sciences Laboratories, Rutgers University, Piscataway, New Jersey, USA

Received 1 August 2001; revised 15 May 2002; accepted 15 May 2002; published 12 March 2003.

[1] Synthetic hysteresis loops were generated by numerically solving the classical Stoner-Wohlfarth model and a thermally activated Stoner-Wohlfarth model for a set of randomly oriented magnetic grains. Although computationally intensive this method allows forward modeling of hysteresis loops of single-domain (SD) and viscous grains. In the classic Stoner-Wohlfarth model the shape of the modeled loops can be modified by changing the distribution of the anisotropy energy but all the loops will all have similar hysteresis parameters M_{sr}/M_s and H_{cr}/H_c corresponding to that of a theoretical assemblage of SD particles. The thermally activated Stoner-Wohlfarth model, which allows the magnetic moment of each grain to switch between two energy minima according to Boltzmann statistics, extends the SD model toward superparamagnetic (SP) grains and introduces a volume dependency. Numerical simulation using the thermally activated model shows that the shapes of SD loops are modified by the effect of the thermal energy if the particles are sufficiently small. The major effect of the thermal disturbance is observed in highly viscous particles (smaller than approximately 0.03 μm in diameter, for magnetite) where it strongly reduces the coercivity and to a lesser extent the remanent magnetization. The effect on the hysteresis parameters is a large increase in H_{cr}/H_c and a decrease in M_{sr}/M_s, by factors that vary with anisotropy distribution, grain volume and measurement time. For certain grain sizes, these result in hysteresis parameters that are similar to those attributed to pseudosingle-domain (PSD) grains. *INDEX TERMS:* 1540 Geomagnetism and Paleomagnetism: Rock and mineral magnetism; 1519 Geomagnetism and Paleomagnetism: Magnetic mineralogy and petrology; 1512 Geomagnetism and Paleomagnetism: Environmental magnetism; 1594 Geomagnetism and Paleomagnetism: Instruments and techniques; 1599 Geomagnetism and Paleomagnetism: General or miscellaneous; *KEYWORDS:* hysteresis loops, Stoner-Wohlfarth model, single domain, thermal activation, superparamagnetic

Citation: Lanci, L., and D. V. Kent, Introduction of thermal activation in forward modeling of hysteresis loops for single-domain magnetic particles and implications for the interpretation of the Day diagram, *J. Geophys. Res.*, *108*(B3), 2142, doi:10.1029/2001JB000944, 2003.

1. Introduction

[2] Numerical modeling of hysteresis loops makes it possible to investigate the magnetic behavior of natural materials. In small, SD particles with homogeneous magnetization where the switch of the magnetic moment occurs as a coherent rotation, the simplest model is that of *Stoner and Wohlfarth* [1948], which also assumes noninteracting particles with uniaxial anisotropy. Despite these stringent assumptions the Stoner-Wohlfarth model constitutes a fundament of SD magnetization theory on which a large part of rock magnetism is constructed. On this basis, *Day et al.* [1977] recognized a practical way to describe hysteresis loops (at least for titanomagnetite) and classify them according to the mean magnetic particle grain size, in the well-known Day plot. It has been observed that the hysteresis parameters of natural samples with a stable magnetization generally do not exhibit the magnetic parameters characteristic of SD particles and most often plot in the PSD field of the Day diagram. Parameters expected for pure SD grains are rarely observed even in synthetically grown crystals with well-controlled grain size where the presence of large grains can be ruled out [*Heider et al.*, 1987]. In many of these cases magnetic interaction between particles [e.g., *Sprowl*, 1990; *Hansen and Morup*, 1998; *Dormann et al.*, 1999; *Muxworthy*, 2001] is acknowledged to explain the observed behavior and this seems to be especially appealing

[1]Now at Istituto di Dinamica Ambientale, University of Urbino, Urbino, Italy.

[2]Also at Lamont-Doherty Earth Observatory of Columbia University, Palisades, New York, USA.

0148-0227/03/2001JB000944$09.00

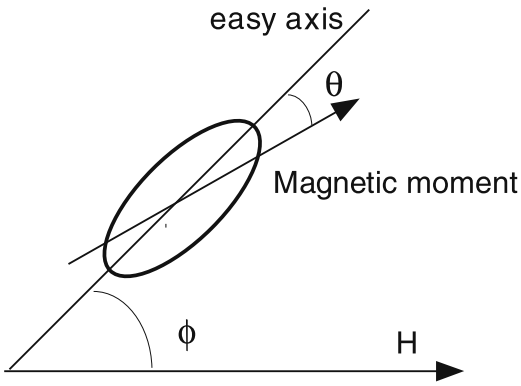

Figure 1. Geometrical description of the elements of the generic Stoner-Wohlfarth particle.

in synthetic samples because of the difficulty to effectively disperse the magnetic grains in the matrix.

[3] Modeling the magnetization as function of the field involves finding the solution to the free energy function of each particle. Even in the simple Stoner-Wohlfarth model, a general analytical solution is not possible and must be achieved numerically. Numerical solutions of the classic Stoner-Wohlfarth model for single particles have long been known, while the solution for an assemblage of randomly oriented particles has been investigated more recently and mostly from an engineering point of view [e.g., *Jiles et al.*, 1992; *Friedman and Mayergoyz*, 1992; *Oliveira de Jesus and Kleemann*, 1997; *Basso and Bertotti*, 2000; *Szabo and Ivanyi*, 2000]. *Tauxe et al.* [1996] investigated the numerical modeling of hysteresis loops from a geological perspective by calculating the hysteresis parameters of mixtures of SP and stable SD grains. In this paper we have added the effect of thermal agitation to a Stoner-Wohlfarth ensemble of magnetic particles and explored numerically its consequences on the magnetization during a hysteresis loop. This approach is substantially different from that of *Tauxe et al.* [1996] because we do not use mixtures of different grain size but investigate the behavior of assemblages of viscous to "near-SP" particles with constant volume. Moreover, the definition of a sharp threshold between SP and stable SD particles is not necessary. We show that PSD-like hysteresis parameters can be obtained in fine particles due only to thermal activation; we also describe hysteresis loops of ensembles of viscous grains near to the stable SD/SP boundary.

2. Theory

2.1. Stoner-Wohlfarth Model

[4] The Stoner-Wohlfarth model assumes noninteracting, SD particles, with uniaxial anisotropy where the switch of the magnetic moment occurs by coherent rotation. In such a magnetic particle the free energy function E is expressed by the sum of the anisotropy and magnetostatic terms [e.g., *Nagata*, 1961; *Stacey and Banerjee*, 1974; *O'Reilly*, 1984; *Dunlop and Özdemir*, 1997; *Bertotti*, 1998]

$$E = v\left(K_u \sin^2\theta - \mu_o, H\, M_s \cos(\theta - \phi)\right), \qquad (1)$$

where v is the particle volume, K_u the anisotropy constant, M_s its spontaneous magnetization and H the magnetic field. The angle ϕ is the orientation of the particle's "easy axis" with respect to the field direction and θ is the angle between the easy axis and the magnetic moment as illustrated in Figure 1. The possible states of the magnetic moment (i.e., its orientations θ) correspond to that of the minima of the energy function $E(\theta)$. Stable states of magnetization result, therefore, from $dE/d\theta = 0$ and $d^2E/d\theta^2 > 0$, while switches of the magnetization occur when the second derivative vanishes (i.e., $d^2E/d\theta^2 = 0$). Each particle's magnetization is represented by the component of its magnetic moment along the field direction and it is given by $M_s\cos\theta$. The parameters K_u, M_s, v and the orientation ϕ, are considered constant for each particle, but these parameters will vary within the assemblage of different particles.

[5] In the most simple case with $H = 0$ (Figure 2a) the energy barriers Eb_1 and Eb_2 will be $Eb_1 = Eb_2 = K_u v$ and $E_{mins}(\theta)$ has a straightforward analytical solution. When $H \neq 0$, analytical solutions exist only for $\phi = \{0, \pi/4, \pi/2\}$ but in the most general case (Figure 2b) the angle θ must be computed numerically by finding the maxima and minima of equation (1).

[6] We may notice that in the Stoner-Wohlfarth model the particle's volume has an influence only on the total magnetization; the behavior of the particle and its magnetization curve are not influenced by the volume changes. In this sense we consider the model volume-independent.

2.2. Thermal Activation

[7] Besides the assumptions mentioned above, the Stoner-Wohlfarth model presumes no thermodynamical effect. This means that the state of a magnetic moment in local minima will remain the same until the field is changed. Such a behavior is strictly true only at absolute zero or in practice if

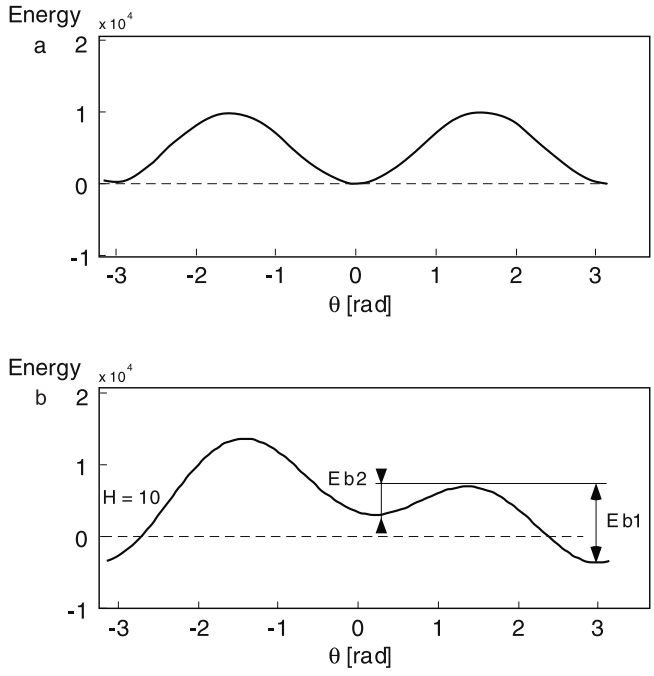

Figure 2. Plot of the free energy function for a Stoner-Wohlfarth (uniaxial) particle from equation (1), in the cases when (a) $H = 0$ and (b) $H \neq 0$. The energy barriers Eb_1 and Eb_2 are also shown.

the thermal energy is very small compared to the energy barriers (i.e., $kT \ll Eb$). In general, however, the magnetization will approach a thermodynamical equilibrium with time due to thermal fluctuations. The analysis of thermal fluctuations of a SD particle is from *Néel* [1949, 1955] and later revised by *Brown* [1959, 1963]. In their model it is assumed that the magnetic moment of a particle can occupy only two possible states, that we call 1 and 2, that correspond to the energy minima of equation (1). For such a bi-state particle the probability of the magnetization being in a given state (e.g., state 1) is described by the so-called kinetic equation [e.g., *Bertotti*, 1998]:

$$\frac{dn_1}{dt} = -n_1 w_1 + n_2 w_2, \tag{2}$$

where n_1 and n_2 are the fractions of magnetization in states 1 and 2, respectively (assuming $n_1 + n_2 = 1$) and $w_{1,2} = f_o \exp(-Eb_{1,2}/kT)$. The $n_1 w_1$ and $n_2 w_2$ terms in equation (2) describe the probability of the magnetic moment to switch from state $1 \rightarrow 2$ and from $2 \rightarrow 1$, respectively, according to Boltzmann statistics. The preexponential proportionality factor f_o represents the atomic reorganization frequency, which is a function of K_u, M_s, T, H and ϕ. Several formulations are reported in the literature [*Brown*, 1959, 1963], here we consider $f_o \approx 1 \times 10^9$, as suggested by *Moskowitz et al.* [1997], and constant, arguing that the exponential terms in equation (2) dominate the variability. After substituting $n_2 = 1 - n_1$ and integrating equation (2) with respect to t, assuming thus T and $Eb_{1,2}$ constant, we obtain the classic expression of the approach to thermal equilibrium [e.g., *Bertotti*, 1998]:

$$n_1(t) = n_{eq} + \left(n_1(0) - n_{eq}\right) \exp\left(\frac{-t}{\tau}\right), \tag{3}$$

where

$$n_{eq} = \frac{w_2}{w_1 + w_2}; \quad \frac{1}{\tau} = w_1 + w_2.$$

The term n_{eq} represents the magnetization at the thermodynamical equilibrium, while $n_1(0)$ is the initial fraction of moments in state 1. Since the relaxation time τ is controlled by the energy barriers $Eb_{1,2}$, thermal activation depends on the particle volume and therefore introduces a volume dependency into the magnetization model. From equation (3), the fractions $n_1(t)$ and $n_2(t) = 1 - n_1(t)$ can be calculated as a function of time t and the net magnetization of the ensemble of particles computed by the vector sum of the moments in the two states.

[8] During hysteresis loop the field H is not constant; therefore the energy barriers $Eb_{1,2}$, and consequently, the relaxation time τ, are also varying as a function of H. In this case equation (3) can still be used with the implicit assumption that the process advances in small steps having constant H. The thermal effect on the magnetization in this case is computed for every successive step, assumed at constant field, taking as the initial state $n_1(0)$ from the previous step. A more elegant solution will include the general case when the terms w_1 and w_2 are functions of time because the energy barrier $Eb_{1,2}$ are variable in t. This is obtained by integrating equation (2) with $w_{1,2}(t)$, which results in

$$n_1(t) = C \exp(\tau') + \exp(\tau') \int w_2(t) \exp(-\tau') dt, \tag{4}$$

where

$$\tau' = -\int w_1(t) + w_2(t) dt \tag{5}$$

and C is an integration constant that depends on the initial conditions. The solution of equation (4) must be obtained numerically. In fact, the functions $w_1(t)$ and $w_2(t)$ and therefore the relative integrals do not have in general an analytical expression, thus they have to be computed for each particle of the assemblage by calculating the energy barriers of the free energy function (equation (1), in the case of Stoner-Wohlfarth particles). However this is not a real disadvantage since such a numerical solution of the free energy equation or the equivalent switching field [*Tauxe et al.*, 1996], is anyhow necessary. The advantage of equation (4) is that the $w_{1,2}$ integrals can be calculated numerically with precise methods [e.g., *Davis and Rabinowitz*, 1984; *Press et al.*, 1992] and there is no need to assume a constant field H during each step as when using equation (3). This gives a higher precision or for a given precision, requires a smaller number of field steps and therefore results in a faster computation. A disadvantage of equation (4) is that the exponential of the τ' integrals is likely to cause a numerical overflow in any calculation where the $w_{1,2}$ factors became too large. This problem can in principle be circumvented by restricting $w_{1,2}$ to a value that is only sufficiently large in the context of the experiment. In our calculation, where we had to keep the field step small to find an accurate solution of the Stoner-Wohlfarth model, we have chosen to use equation (3) in the bulk computation to keep the program algorithm simple and used equation (4) to check the results in a few selected cases.

[9] It should be remembered at this point that computing the magnetization for a set of nonidentical particles implies that $n_{1,2}$ are not only function of time but, more generally, $n_{1,2}(t, K_u, v, H, T, \phi)$.

2.3. Limits of the Thermal Activation Model

[10] The assumptions used to simplify the model define the limits of its applicability. As stated before, the model assumes noninteracting SD particles with uniaxial anisotropy. In the case of a highly magnetic mineral like magnetite, this limits the use of the model to assemblages where the anisotropy is controlled by the particle's shape. This is probably the case for most detrital magnetite but may not be the case, for instance, for magnetite particles in oceanic basalt glass that are known to have cubic anisotropy [*Gee and Kent*, 1995].

[11] The range of particle grain sizes is limited on one side by the thermal activation model and on the other by the assumption of coherent rotations. Thermal activation assumes that the magnetic moment of a particle can occupy only two orientations (bi-state particles). This is appropriate when the thermal energy is smaller than the anisotropy energy but it is not appropriate when $kT \geq K_u v$ and the

probability to assume any orientation is nonnegligible. In such a case, and particularly when $kT \gg K_u v$, the grains become truly SP and their magnetization curve is better described by a Langevin function [e.g., *Tauxe et al.*, 1996; *Dunlop and Özdemir*, 1997]. At room temperature this restricts the grain size of the particles to a minimum volume of about 1×10^{-24}m^3 (corresponding to a size of about 0.01 μm for a cubic particle). These small particles may have a very short relaxation time and behave like SP at room temperature although their magnetization cannot be described by a Langevin function because the prerequisite $kT \gg K_u v$ is not met.

[12] On the opposite side the assumption of coherent rotations limits the maximum grain size of the particles. For magnetite this limit is set between 0.07 and 0.1 μm on the basis of micromagnetic calculations [*Winkelhofer et al.*, 1997; *Newell and Merrill*, 2000b]; above this size the switch of the particle's magnetic moment occur with more energetically favorable configurations than coherent rotations and they do not behave like SD. Magnetite has therefore a relatively narrow range of grain size in which the model is adequate. Finally, the assumption of the absence of magnetic interaction between particles might give further restriction to the applicability of the model.

3. Numerical Modeling

[13] The solution of the nonthermally activated model requires finding the orientation θ of the local energy minima of function $E(\theta)$ in each particle, while varying the field H. The field is changed in small steps such that subsequent energy minima will also have a small difference in orientation θ. Therefore, when the function $E(\theta)$ has two local minima the magnetic moment will be found in the one that has θ closer to that of the previous field. Switches of the magnetic moment (i.e., coherent rotations) may occur when the magnetostatic term becomes large enough to meet the condition $dE^2/d^2E = 0$ and the energy barrier is reduced to zero.

[14] A typical run involves computing the directions θ corresponding to the local energy minima of the magnetic moments in a set of randomly oriented particles with the same K_u. The calculation starts from a field large enough to saturate the ensemble of particles, which is then decreased in small steps to zero and increased again in the opposite direction. The maximum field used in the calculations was 500 mT with increments of 2 mT. With such small increments, no practical differences were found between equations (3) and (4) in the calculation of the thermal relaxation. Using this approach the ascending and descending parts of the loops are computed at once. The initial magnetization curve can also be calculated starting from a configuration with randomly oriented moments and increasing the field from zero.

[15] The thermal agitation is introduced in the model either using equation (3) applied at each field during the magnetization process, or using equation (4). Because of the assumption of bi-state particles we are only interested in the value of the energy barriers $Eb_{1,2}$ and not in the shape of the function $E(\theta)$, therefore it is solely necessary to search for the two energy minima corresponding to the states 1 and 2 and the maximum separating them. A constant representing the time elapsed during the experiment must be allowed; here we made an analog with a real measurement (often made on an alternating gradient force magnetometer) and used a Δt of 1 sec at each field step, corresponding to a time of a few minutes for the full cycle. The effect of using a slightly different measurement time will be that of a shift in the grain volume, which can be considered a minor problem since the evaluation of precise values of the particle volume are affected by the scarce knowledge of the preexponential factor f_o that can vary by a factor of 10 according to the different estimates.

[16] For the purpose of searching for the minima and maxima of E it was found that the most practical approach was an exhaustive search. Minima and maxima were searched using the first derivative of $E(\theta)$ that were solved over their entire domain $(0-2\pi)$ with a 100 point grid. Precise solutions were calculated by interpolation. In this particular problem, where the functions are known to be smooth with 2 or 4 solutions and their domain is finite, this simple algorithm was found to be faster than more complex zero-finding routines. Moreover the method has the advantage that it gives all the solutions at once and therefore the energy barriers are obtained with little additional calculations.

[17] Simple hysteresis loops are obtained by vector sum of the individual contributions of a large number of particles with uniformly distributed orientations φ, a given anisotropy constant K_u and volume v. This procedure is then repeated several times for each anisotropy constant and volume. The actual loops are the sum of simple loops calculated for different distributions of K_u and a given volume.

[18] In our calculation we used parameters typical for magnetite with a $M_s = 4.8 \times 10^5$Am^{-1} and a set of 10,000 particles with 100 different K_u corresponding to microcoercivities ($H_K = 2K_u/M_s$) ranging from about 10 to 300 mT. This range includes the minimum and maximum theoretical values for magnetite calculated for shape anisotropy, which is appropriate for the magnetostatic energy term in the Stoner-Wohlfarth model. The whole coercivity range is not necessarily used in each loop since the contribution to actual coercivity of each assemblage of grains is determined by the K_u distribution function. In our experiment we assumed a lognormal K_u distribution defined by the central point μ, and the dispersion σ, which are the analog of the mean and standard deviation in the normal (Gaussian) distribution. A lognormally distributed K_u have been used because it seems to be a reasonable approximation of the coercivity distribution observed in many natural samples [*Robertson and France*, 1994]. We experimented different parameters μ and σ (Figure 3a), which were designed to have a mean coercivities similar to those normally observed in natural samples. The contribution of the extreme values of coercivity to the whole ensemble coercivity, although variable, remains small. The loops are calculated for a temperature of 300K and volumes ranging from 3×10^{-24} to 1×10^{-21}m^3, corresponding to sizes (for cubic particles) ranging from 0.014 to 0.1 μm.

[19] Once the loops are computed, the calculations of the saturation magnetization M_s, the saturation remanent magnetization M_{sr} and of the coercivity H_c are straightforward. Determining the coercivity of remanence H_{cr} would require

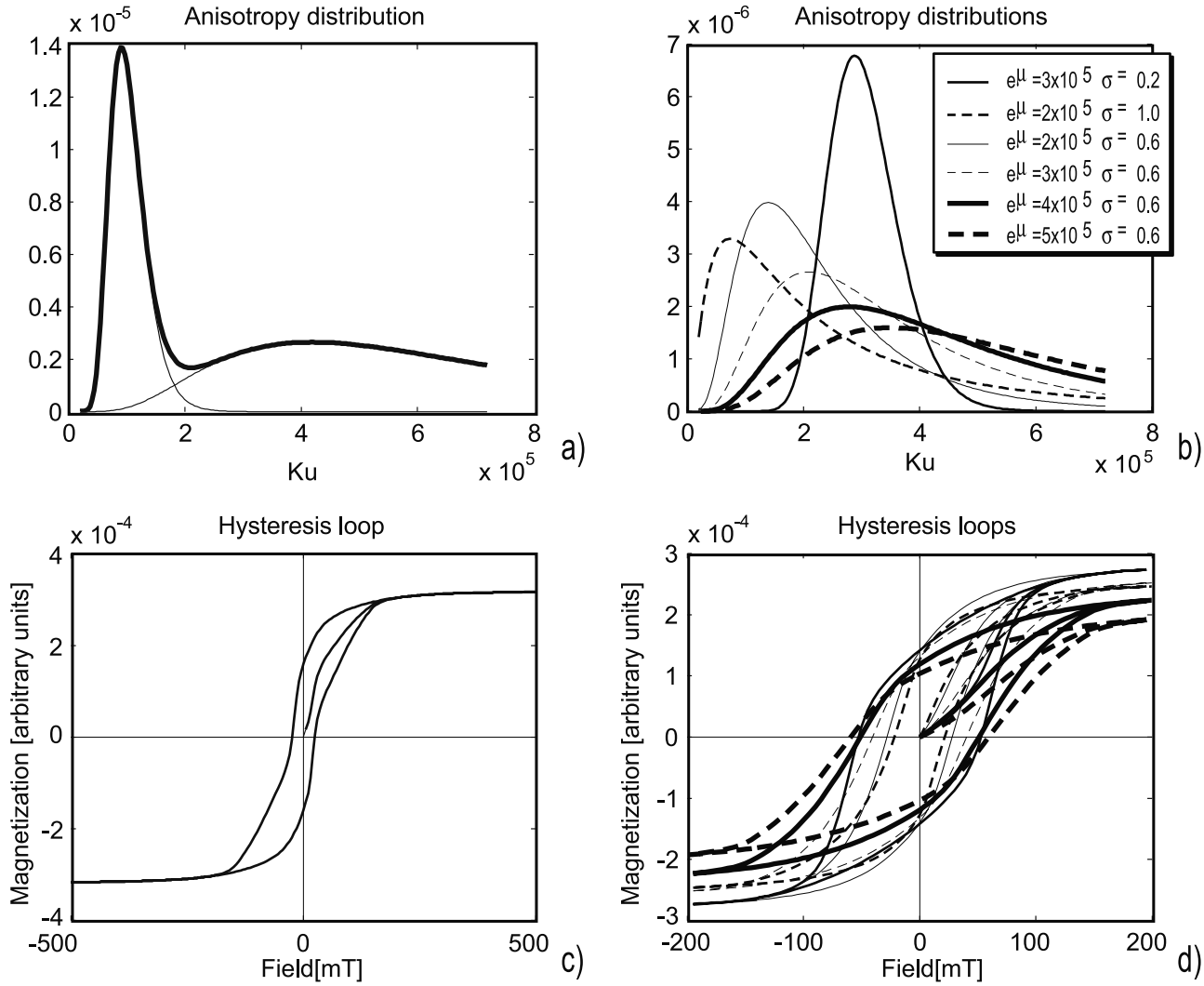

Figure 3. Nonthermally activated loops of an ensemble of randomly oriented Stoner-Wohlfarth particles. The different anisotropy (K_u) distributions shown in Figure 3a correspond to the different loops' shapes shown in Figure 3b. The μ parameter is shown as *exp*(μ), which corresponds to the actual mean; the initial magnetization is calculated starting from an assemblage of randomly oriented magnetic moments. A constricted loop obtained with a bimodal K_u distribution in Figure 3c is also shown in Figure 3d.

modeling the backfield demagnetization and dealing with the different time constants of the new measurement, instead we calculated H_{cr} directly from the synthetic hysteresis loop using the "ΔM curve" of *Tauxe et al.* [1996] or the equivalent method proposed by *Fabian and von Dobeneck* [1997], that give a sufficient approximation. With this method H_{cr} is computed by calculating the field corresponding to the median value of the "ΔM curve", which is obtained as the difference between the ascending and descending loops. Calculation using actual hysteresis loops from various rock types confirm that H_{cr} computed from the ΔM curve are practically identical to those computed with the classic method from backfield demagnetization.

4. Results and Discussion

[20] In the Stoner-Wohlfarth model the shape of the hysteresis loop is independent of grain volume, which affects only the total magnetization M_s and M_{sr}, as long as it remains in the appropriate (SD) grain size range. The shape of the loops can instead be modeled by mixing populations of grains with different anisotropy constants K_u (or corresponding microcoercivities H_K). In our experiment we assumed a lognormal K_u distribution but this mixing model would work as well with any theoretical or empirical distribution. Some of the different hysteresis loops obtained with different K_u distributions are illustrated in Figure 3b, including a constricted loop created using a bimodal distribution (Figures 3c and 3d). Despite their differences the hysteresis parameters of all these loops are still that of theoretical SD particles with only minor variation of H_{cr}/H_c due to the varying K_u distribution (Figure 4). In particular the H_{cr}/H_c ratio of the ensemble with the narrower distribution of K_u is very close to the theoretical value of 1.09, calculated for a single coercivity, reassuring on the method used in calculating H_{cr}. The similarity between the hysteresis

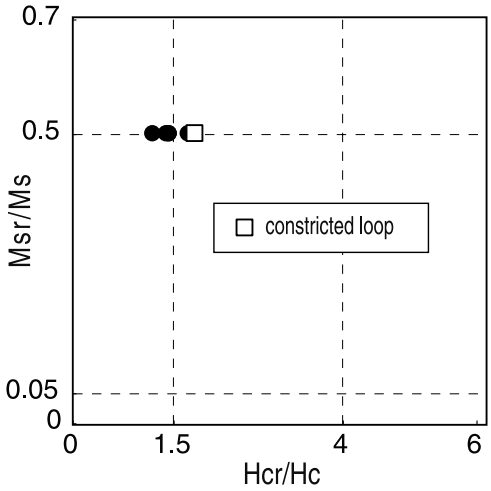

Figure 4. Hysteresis parameters of the loop depicted in Figures 3b and 3d. The small variation of the H_{cr}/H_c is a consequence of the different anisotropy distributions.

parameters have to be considered a feature of the Day plot rather than a pitfall because it aims to identify the SD particles independently from their anisotropy distribution and in this respect it seems very successful.

[21] The introduction of a thermodynamic effect in the Stoner-Wohlfarth model allows the prediction of the hysteresis parameters of fine particles as a function of their volume and anisotropy distribution. The major effect of thermal agitation on a simple hysteresis loop of a set particles with randomly oriented axis and specific volume and K_u is a reduced coercivity due to the effect known as the fluctuating field [*Dunlop*, 1976; *Dunlop and Ödzemir*, 1997]. When particles with different anisotropy constants are mixed (using again a lognormal distribution as shown in Figure 5a), we obtained loops with varying shapes and hysteresis parameters (Figures 5b, 5c, and 5d). The parameters' variability is mostly controlled by the grain volume, but since the energy barriers are also a function of the grain anisotropy, the K_u distribution has also an important influence. As shown in the Day plots (Figures 6a, 6b, 6c, and 6d), thermal agitation has a larger effect on the coercivity H_c

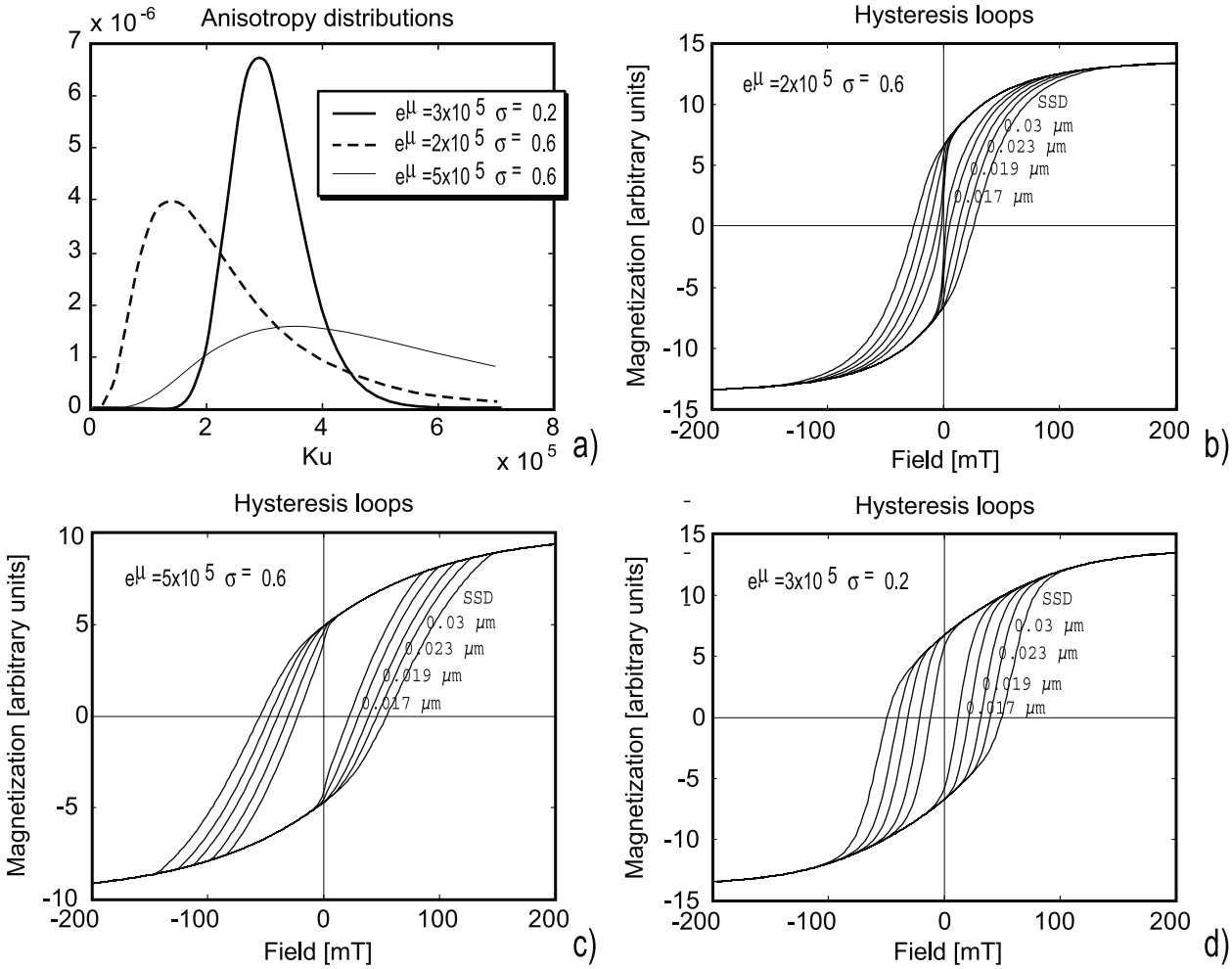

Figure 5. Thermally activated loops (Figures 5b, 5c, and 5d) of an ensemble of randomly oriented Stoner-Wohlfarth particle with the different anisotropy distributions shown in Figure 5a, and different grain sizes calculated as cubic root of the volume.

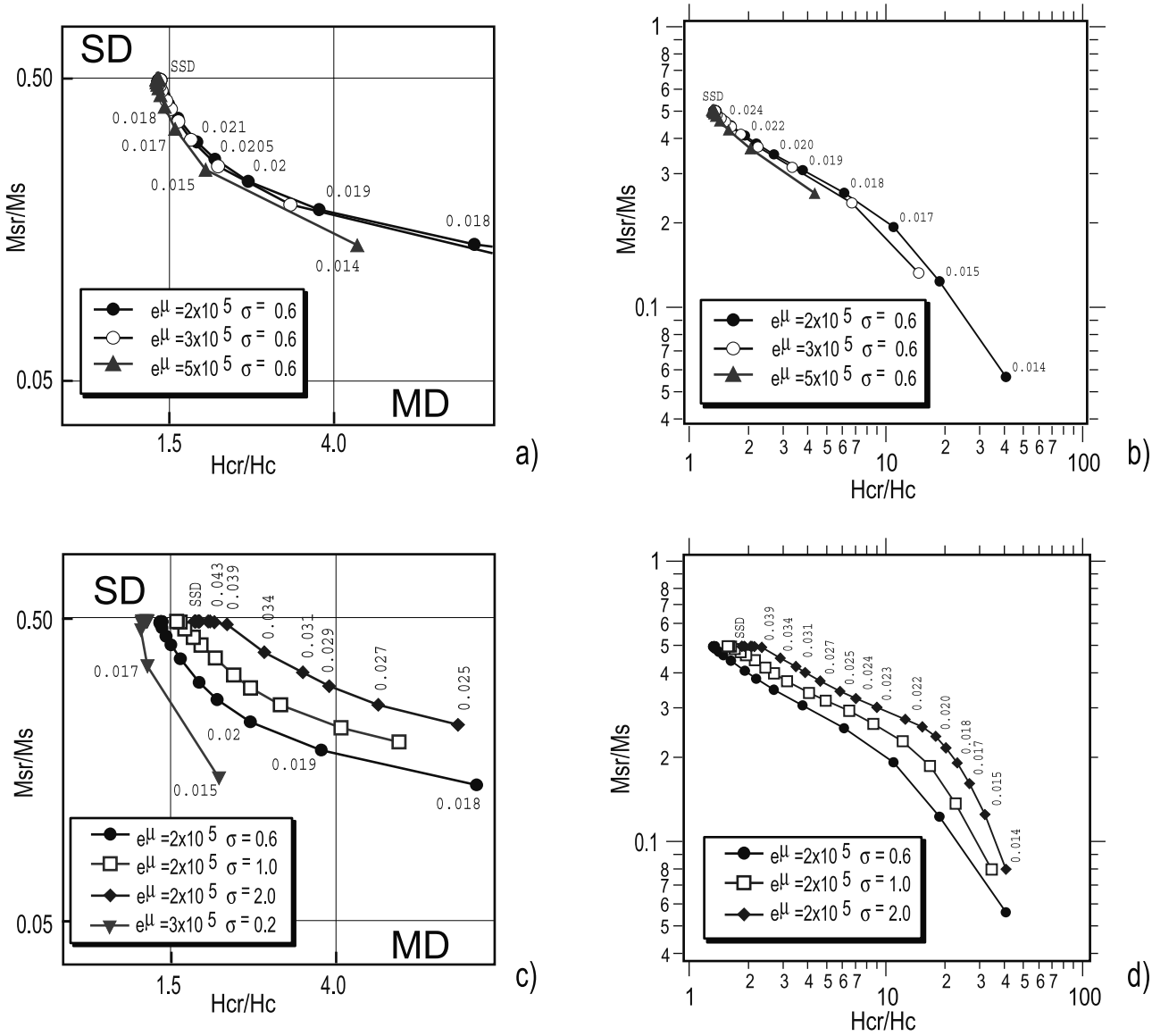

Figure 6. Hysteresis parameters for thermally activated loops with different volumes and anisotropy (K_u) distributions. Shown in Figures 6a and 6c are classic Day plots with linear scales and plotted on a log-log scale in Figures 6b and 6d. The variations in the parameters induced by a change of the dispersion (σ) of the anisotropy distribution are shown in Figures 6c and 6d, whereas Figures 6a and 6b show the effect of varying the central value (μ) of the anisotropy distribution.

compared to the coercivity of remanence H_{cr} and as a consequence the H_{cr}/H_c ratio can change appreciably. M_{sr} is also decreased by the fraction of grains that are "relaxed" by thermal fluctuations and this reduces the M_{sr}/M_s ratio. In the smallest particles that have been modeled this effect is extreme, and they may exhibit a SP-like behavior with very low M_{sr}/M_s ratios. In larger particles, it is observed that the variation of the M_{sr}/M_s ratio is proportionally smaller than the H_{cr}/H_c ratio.

[22] In the thermally activated model the K_u distribution has a much larger influence on the hysteresis compared to the nonthermally activated model. The effect of the volume variations and of the different K_u distributions is shown in Figure 6, in which the markers corresponding to ensembles with the same K_u distribution and different volumes are connected with a line. The variation of the central value μ of the K_u distributions results in a change of the average anisotropy of the ensemble, and therefore of its average energy barrier. This effect produce an effect on the hysteresis parameters similar to that of a volume variation and can be observed in the overlapping trends shown of Figures 6a and 6b (top two panels). The dispersion parameter σ is more effective in changing the loops shape and its variation results in different trends showed in Figures 6c and 6d (lower two panels).

[23] For magnetite the range of grain size that is affected by thermal relaxation, at room temperature and with time a constant compatible with actual laboratory measurements, corresponds to that of viscous to "near-SP" grains, approximately. 0.015–0.03 μm in size. These values can be

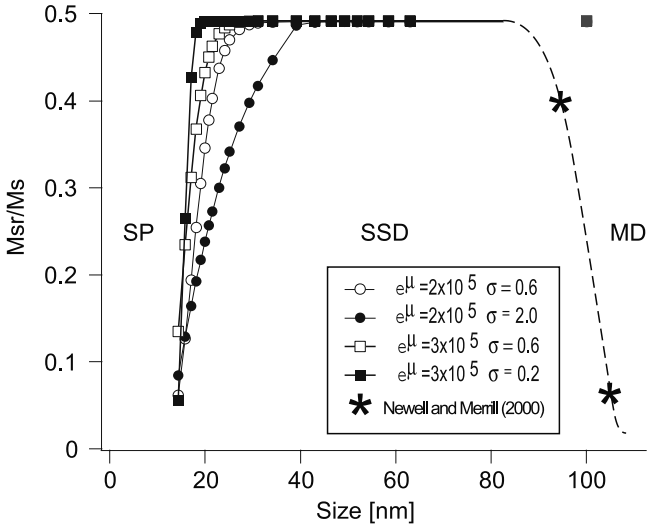

Figure 7. Hysteresis parameters M_{sr}/M_s plotted versus grain size showing the range where the thermal activation is effective in changing the magnetic behavior of fine particles. Calculation was made up to a size of 100 nm that also gives $M_{sr}/M_s = 0.5$ but we take the upper limit of the stable SD/MD as a rather sharp transition slightly below 100 nm (dashed line) according to the calculation of *Newell and Merrill* [2000a, 2000b].

changed roughly by a factor of 2 assuming a different preexponential factor f_o. Stable SD particles are obviously not affected by the thermal relaxation at this timescale, but it seems that they are restricted to the rather narrow grain size range of about 0.03–0.07 μm according to the calculations of *Winkelhofer et al.* [1997] and the experimental measurements of *Dunlop* [1973]. A slightly larger range is suggested by the calculation of *Newell and Merrill* [2000a, 2000b], who suggest an upper limit for stable SD particles of 0.1 μm and a sharp transition between SD and multidomain (MD) with no real PSD grains. This is illustrated in Figure 7 by plotting the M_{sr}/M_s ratio versus (cubic) particles size.

[24] The collective results from our calculation, including all the various grain size and K_u distributions, are plotted in Figure 8 together with some available experimental data. The H_{cr}/H_c ratio can reach very large values (up to 40 in our calculations) in the smaller particles whereas the M_{sr}/M_s ratio usually remains above that of MD grains and reaches similar low values only in extreme cases. This defines an SP-SD trend, shown in Figure 8, which is distinct from that expected in PSD/MD grains [*Dunlop*, 1986] and that may thus be useful to distinguish magnetic particles at the opposite extremes of the grain size range. Hysteresis data and trends from submarine basaltic glasses and chilled margins [*Tauxe et al.*, 1996; *Gee and Kent*, 1999], which are expected to have very fine magnetic grain sizes, tend to fall along our calculated stable SD-SP trend (although the magnetic carrier in this material may not be an appropriate analog of our model due to the apparent prevalence of cubic anisotropy in oceanic basalts [*Gee and Kent*, 1995]). Also shown in Figure 8 is the trend of hysteresis data for remagnetized North American limestones which has also been interpreted as due to a mixture of stable SD and SP grains [*Jackson*, 1990]. In spite of the model's limits and the uncertainties in grain size and the origin of the anisotropy in the experimental data, we believe that there is a good agreement between the experimental data and the theoretical results, which supports the applicability of our calculations.

5. Conclusions

[25] Our calculations based on the simple Stoner-Wohlfarth model show that a wide range of hysteresis parameters can be obtained when the thermal effect on the magnetization is incorporated in the model. We have also shown that there is a relatively wide range of these viscous SD particles that have parameters falling in the PSD field of the Day plot. Theoretical calculations agree well with experimental results from natural samples of submarine basaltic glasses where there is some control on relative grain size. These calculations also support the interpretation of *Jackson* [1990] that remagnetized North American limestones represent a mixture of stable SD and SP grains. Since both the particle volume and the distribution of particle anisotropy affect the hysteresis parameters, it is not possible to associate unequivocally the parameters with the volume of very small particles. Accordingly, and given the variability of measurement time and the uncertainty of the preexponential factor f_o, the grain size values showed in Figures 6 and 7 should be only considered indicative. Despite these limitations our numerical simulations show a trend of hysteresis parameters that remains well defined in the Day plot even using relatively extremes parameters in the Ku distribution. The stable SD-SP trend defined by our calculations (Figure 8) is distinct from that expected in PSD/MD grains and suggests that Day parameters may be effective in distinguishing

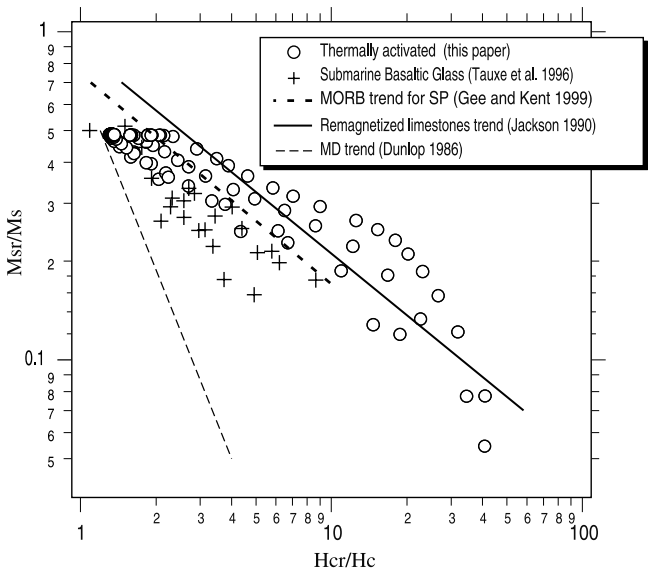

Figure 8. Comparison of hysteresis parameters for thermally activated loops calculated here and experimental data from submarine basaltic glass [*Tauxe et al.*, 1996], MORB trend for SP [*Gee and Kent*, 1999], remagnetized limestones trend [*Jackson*, 1990], and PSD/MD trend [*Dunlop*, 1986].

magnetic particles at the opposite extremes of the grain size range.

[26] The size of stable particles appears to be restricted to a rather narrow grain size range at room temperature (for magnetite) and it seems very likely that any real "SD" sample will be affected by some contribution either from viscous and/or from PSD and MD grains. It is not surprising, therefore, that theoretical stable SD parameters are seldom measured.

[27] **Acknowledgments.** The paper greatly benefited from reviews by David Dunlop, Mike Jackson, and Lisa Tauxe. This work was supported by grants from the U.S. National Science Foundation. Lamont-Doherty Earth Observatory contribution 6303.

References

Basso, V., and G. Bertotti, Hysteresis in soft magnetic materials, *J. Magn. Magn. Mater.*, *215–216*, 1–5, 2000.

Bertotti, G., *Hysteresis in Magnetism for Physicists, Material Scientist and Engineers*, 543 pp., Academic, San Diego, Calif., 1998.

Brown, W. F., relaxation behavior of fine magnetic particles, *J. Appl. Phys.*, *30*, 130–132, 1959.

Brown, W. F., Thermal fluctuation of a single domain particle, *Phys. Rev.*, *130*, 1677–1686, 1963.

Davis, P., and P. Rabinowitz, *Method of Numerical Integration*, 2nd ed., 612 pp., Academic, San Diego, Calif., 1984.

Day, R., M. Fuller, and V. A. Schmidt, Hysteresis parameters of titanomagnetite: Grain size and compositional dependence, *Phys. Earth Planet. Inter.*, *13*, 260–267, 1977.

Dormann, J. L., D. Fiorani, and E. Tronc, On the model for interparticle interaction in nanoparticle assemblies: Comparison with experimental results, *J. Magn. Magn. Mater.*, *202*, 251–267, 1999.

Dunlop, D. J., Superparamagnetic and single-domain threshold sizes in magnetite, *J. Geophys. Res.*, *78*, 1780–1793, 1973.

Dunlop, D. J., Thermal fluctuation analysis: A new technique in rock magnetism, *J. Geophys. Res.*, *81*, 3511–3517, 1976.

Dunlop, D. J., Hysteresis properties of magnetite and their dependence on particle size: A test of pseudo-single-domain remanence models, *J. Geophys. Res.*, *91*, 9569–9584, 1986.

Dunlop, D. J., and Ö. Ödzemir, *Rock Magnetism: Fundamentals and Frontiers*, 573 pp., Cambridge Univ. Press, New York, 1997.

Fabian, K., and T. von Dobeneck, Isothermal magnetization of samples with stable Preisach function: A survey of hysteresis,remanence, and rock magnetic parameters, *J. Geophys. Res.*, *102*, 17,659–17,677, 1997.

Friedman, G., and I. D. Mayergoyz, Stoner-Wohlfarth hysteresis model with stochastic input as a model of viscosity in magnetic material, *IEEE Trans. Magn.*, *28*, 2262–2264, 1992.

Gee, J., and D. V. Kent, Magnetic hysteresis in young mid-ocean ridge basalts: Dominant cubic anisotropy?, *Geophys. Res. Lett.*, *22*, 551–554, 1995.

Gee, J., and D. V. Kent, Calibration of magnetic granulometric trend in oceanic basalts, *Earth Planet. Sci. Lett.*, *170*, 377–390, 1999.

Hansen, H. F., and S. Morup, Models for the dynamics of interacting magnetic nanoparticles, *J. Magn. Magn. Mater.*, *184*, 262–274, 1998.

Heider, F., D. J. Dunlop, and N. Sugiura, Magnetic properties of hydrothermally recrystallized magnetite crystals, *Science*, *236*, 1287–1290, 1987.

Jackson, M., Diagenetic source of stable remanence in remagnetized Paleozoic cratonic carbonates: A rock magnetic study, *J. Geophys. Res.*, *95*, 2753–2762, 1990.

Jiles, D. C., J. B. Thoelke, and M. K. Devine, Numerical determination of hysteresis parameters for the modeling of magnetic properties using the theory of ferromagnetic hysteresis, *IEEE Trans. Magn.*, *28*, 27–35, 1992.

Moskowitz, B. M., R. B. Frankel, S. A. Walton, D. P. E. Dickson, K. K. W. Walton, T. Douglas, and S. Mann, Determination of the preexponential frequency factor for superparamagnetic maghemite particles in magnetoferritin, *J. Geophys. Res.*, *102*, 22,671–22,680, 1997.

Muxworthy, A. R., Effect of grain interactions on the frequency dependence of magnetic susceptibility, *Geophys. J. Int.*, *144*, 441–447, 2001.

Nagata, T., *Rock Magnetism*, 350 pp., 2nd ed., Maruzen, Tokyo, 1961.

Nèel, L., Thèorie du trainage magneétiquedes feromagnétiques en grains fins avec applications aux teres cuites, *Ann. Géophys.*, *5*, 99–136, 1949.

Nèel, L., Some theoretical aspect of rock magnetism, *Adv. Phys.*, *4*, 191–243, 1955.

Newell, A. J., and R. T. Merrill, Nucleation and stability of ferrimagnetic states, *J. Geophys. Res.*, *105*, 19,337–19,391, 2000a.

Newell, A. J., and R. T. Merrill, Size-dependent of hysteresis properties of small pseudo-single domain grains, *J. Geophys. Res.*, *105*, 19,393–19,403, 2000b.

Oliveira de Jesus, J. C., and W. Kleemann, The magnetization reversal in uniaxial model ferromagnet, *J. Magn. Magn. Mater.*, *169*, 159–168, 1997.

O'Reilly, W., *Rock and Mineral Magnetism*, 220 pp., Chapman and Hall, New York, 1984.

Press, W. H., S. A. Teukosky, W. T. Vetterling, and B. P. Flannery, *Numerical Recipes in C: The Art of Scientific Computing*, 2nd ed., 994 pp., Cambridge Univ. Press, New York, 1992.

Robertson, D. J., and D. E. France, Discrimination of remanence-carrying minerals in mixtures, using isothermal remanent magnetisation acquisition curves, *Phys. Earth Planet. Inter.*, *82*, 223–234, 1994.

Sprowl, D., Numerical estimation of interactive effect in single domain magnetite, *Geophys. Res. Lett.*, *17*, 2009–2012, 1990.

Stacey, F. D., and S. Banerjee, *The Physical Principle of Rock Magnetism*, 195 pp., Elsevier Sci., New York, 1974.

Stoner, E. C., and E. P. Wohlfarth, A mechanism of magnetic hysteresis in heterogeneous alloys, *Philos. Trans. R. Soc., Ser. A*, *240*, 599–642, 1948.(Reprinted in *IEEE Trans. Mag.*, 27, 34–75, 1991.)

Szabò, Z., and A. Ivànyi, Computer aided simulation of Stoner-Wohlfarth model, *J. Magn. Magn. Mater.*, *215–216*, 33–36, 2000.

Tauxe, L., T. A. T. Mullender, and T. Pick, Pot-bellies, wasp-waists and superparamagnetism in magnetic hysteresis, *J. Geophys. Res.*, *101*, 571–583, 1996.

Winkelhofern, M., K. Fabiann, and F. Heider, Magnetic blocking temperatures of magnetite calculated with a three-dimensional micromagnetic model, *J. Geophys. Res.*, *102*, 22,695–22,709, 1997.

D. V. Kent, Paleomangnetics Laboratory, Lamont-Doherty Geological Observatory, 61 Route 9W, Palisades, NY 10964-0190, USA. (dvk@ldeo.columbia.edu)

L. Lanci, Istituto di Dinamica Ambientale, University of Urbino, I-61100 Urbino, Italy. (llanci@llanci@uniurb.it)